OPEN

Dominance of Tau Burden in Cortical Over Subcortical Regions Mediates Glymphatic Activity and Clinical Severity in PSP

Jung-Lung Hsu, MD, PhD,†‡§ Yi-Chia Wei, MD, PhD,‡||¶ Ing-Tsung Hsiao, PhD,**††*
*Kun-Ju Lin, MD, PhD,**†† Tzu-Chen Yen, MD, PhD,‡‡ Chin-Song Lu, MD,§§*
*Han-Cheng Wang, MD,||||¶¶ Alexander Leemans, PhD,****
Yi-Hsin Weng, MD, PhD,†‡††† and Kuo-Lun Huang, MD†‡

Downloaded from http://journals.lww.com/nuclearmed by BhDMf5ePHKav1zEoum1tQfN4a+kJLhEZgbsIHo4XMi0hCywCX1AWnYQp/IlQrHD3i3D0OdRyi7TvSFl4Cf3VC4/OAVpDDa8K2+Ya6H515kE= on 04/11/2024

Background: Progressive supranuclear palsy (PSP) is a tauopathy that involves subcortical regions but also extends to cortical areas. The clinical impact of different tau protein sites and their influence on glymphatic dysfunction have not been investigated.

Patients and Methods: Participants (n = 55; 65.6 ± 7.1 years; 29 women) with PSP (n = 32) and age-matched normal controls (NCs; n = 23) underwent ^{18}F-Florzolotau tau PET, MRI, PSP Rating Scale (PSPRS), and Mini-Mental State Examination. Cerebellar gray matter (GM) and parametric estimation of reference signal intensity were used as references for tau burden measured by SUV ratios. Glymphatic activity was measured by diffusion tensor image analysis along the perivascular space (DTI-ALPS).

Results: Parametric estimation of reference signal intensity is a better reference than cerebellar GM to distinguish tau burden between PSP and NCs. PSP patients showed higher cortical and subcortical tau SUV ratios than NCs ($P < 0.001$ and <0.001). Cortical and subcortical tau deposition correlated with PSPRS, UPDRS, and Mini-Mental State Examination scores (all P's < 0.05). Cortical tau deposition was further associated with the DTI-ALPS index and frontal-temporal-parietal GM atrophy. The DTI-ALPS indexes showed a significantly negative correlation with the PSPRS total scores ($P < 0.01$). Finally, parietal and occipital lobe tau depositions showed mediating effects between the DTI-ALPS index and PSPRS score.

Conclusions: Cortical tau deposition is associated with glymphatic dysfunction and plays a role in mediating glymphatic dysfunction and clinical severity. Our results provide a possible explanation for the worsening of clinical severity in patients with PSP.

Key Words: glymphatic activity, progressive supranuclear palsy, ^{18}F-Florzolotau

(*Clin Nucl Med* 2024;49: 387–396)

BACKGROUND

Tauopathy in Progressive Supranuclear Palsy

Progressive supranuclear palsy (PSP) is a rare form of tauopathy that is composed predominantly of the 4-repeat form of tau.[1] Core clinical features include ocular motor dysfunction, postural instability, akinesia, and cognitive dysfunction.[2] Typical and diverse clinical phenotypes, such as PSP–Richardson syndrome, PSP–progressive gait freezing (PSP-PGF), PSP–cerebellar ataxia, and PSP–speech/language disorder, have been reported in the literature.[2] Although there are many clinical phenotypes, the diagnosis of PSP is based on the presence of neurofibrillary tangles in subcortical nuclei under neuropathologic examination, and these tangles can be visualized by the recently developed technique, in vivo tau PET imaging.[3,4] Several studies have shown that second-generation tau PET tracers could improve diagnostic accuracy and allow tracking of tau accumulation in PSP.[5,6] Patients with PSP can be identified through the use of MRI, which reveals typical midbrain atrophy with a so-called hummingbird sign in the sagittal plane, as well as various regional brain atrophy.[7] MRI has identified different spatiotemporal patterns of cortical and subcortical atrophic profiles in PSP.[8] In addition, a recent study using tau PET identified 2 distinct progression patterns of tau trajectories in PSP.[9]

The glymphatic system is a waste clearance system, and glymphatic dysfunction has been proposed as a final common pathway for the accumulation of pathological proteins leading to clinical symptoms in primary neurodegenerative diseases.[10] Several studies have demonstrated impairment of the human glymphatic system in subcortical diseases, such as PSP, Parkinson disease (PD), and corticobasal syndrome.[11–13] In the past, an animal study revealed impaired glymphatic function and clearance of tau in an Alzheimer

Received for publication December 6, 2023; revision accepted January 8, 2024.
From the *Department of Neurology, New Taipei Municipal TuCheng Hospital, New Taipei City; †Department of Neurology, Neuroscience Research Center, Linkou Chang Gung Memorial Hospital; ‡College of Medicine, Chang-Gung University, Taoyuan; §Graduate Institute of Mind, Brain, and Consciousness, Taipei Medical University, Taipei; ||Department of Neurology, and ¶Community Medicine Research Center, Chang Gung Memorial Hospital, Keelung; **Department of Nuclear Medicine and Center for Advanced Molecular Imaging and Translation, Linkou Chang Gung Memorial Hospital; ††Department of Medical Imaging and Radiological Sciences and Healthy Aging Research Center, Chang Gung University, Taoyuan; ‡‡APRINOIA Therapeutics, Taipei; §§Professor Lu Neurological Clinic, Taoyuan; ||||Department of Neurology, Shin Kong Wu Ho-Su Memorial Hospital; ¶¶College of Medicine, National Taiwan University, Taipei, Taiwan; ***Image Sciences Institute, University Medical Center Utrecht, Utrecht, the Netherlands; and †††Neuroscience Research Center, Linkou Chang Gung Memorial Hospital, Taoyuan, Taiwan.
Author contributions: J.L.H. and Y.C.W. contributed to the conception and design of the study; Y.H.W., K.J.L., I.T.H., K.L.H., C.S.L., and T.C.Y. contributed to the acquisition and analysis of the data; H.C.W. contributed to manuscript suggestion, and J.L.H. and Y.C.W. contributed to the drafting of the text or preparation of the figures.

Conflicts of interest sources of funding: T.C.Y. owns equity in APRINOIA Therapeutics. The other authors declare no conflicts of interest.

Data availability: All data and algorithms used in this study are included in the manuscript and will be available upon request.
Correspondence to: Kuo-Lun Huang, MD, Department of Neurology, Neuroscience Research Center, Linkou Chang Gung Memorial Hospital, Linkou, Taoyuan, Taiwan. E-mail: drkuolun@cgmh.org.tw; or Yi-Hsin Weng, Department of Neurology, Neuroscience Research Center, Linkou Chang Gung Memorial Hospital, Linkou, Taoyuan, Taiwan. E-mail: yhweng2488@gmail.com.
Supplemental digital content is available for this article. Direct URL citation appears in the printed text and is provided in the HTML and PDF versions of this article on the journal's Web site (www.nuclearmed.com).
Copyright © 2024 The Author(s). Published by Wolters Kluwer Health, Inc. This is an open-access article distributed under the terms of the Creative Commons Attribution-Non Commercial-No Derivatives License 4.0 (CCBY-NC-ND), where it is permissible to download and share the work provided it is properly cited. The work cannot be changed in any way or used commercially without permission from the journal.
ISSN: 0363-9762/24/4905–0387
DOI: 10.1097/RLU.0000000000005141

Downloaded from http://journals.lww.com/nuclearmed by BhDMf5ePHKav1zEoum1tQfN4a+kJLhEZgbsIHo4XMi0hCywCX1AWnYQp/IlQrHD3i3D0OdRyi7TvSFl4Cf3VC4/OAVpDDa8K2+Ya6H515kE= on 04/11/2024

disease (AD) model.[14] Recently, our study showed that glymphatic activity mediates the associations between the cortical deposition of tau and cognitive dysfunction in patients with AD.[15] In primarily subcortical neurodegenerative disorders, one animal study has shown a close interaction between the aquaporin-4 (AQP4)–mediated glymphatic system and parenchymal alpha-synuclein deposition in a model of PD.[16] The role of the glymphatic system in tau deposition in other subcortical diseases remains largely unknown. Because tau deposition in PSP may occur in subcortical nuclei as well as in different cortical regions, it provides an opportunity to investigate the relationships between tau deposition in different brain regions, glymphatic dysfunction, and clinical symptoms in vivo. The aim of the present study was to investigate the associations of topographic distributions of tau burden with diffusion tensor imaging (DTI)–derived glymphatic activity, cortical atrophy, and clinical parameters in patients with PSP.

PATIENTS AND METHODS

This was a cross-sectional study conducted at Linkou Chang Gung Memorial Hospital. The study protocol was approved by the Institutional Review Board (CGMHIRB No. 202002292A0 and 202102215A0). Written informed consent was obtained from each participant before the study procedure. Each participant completed a cognitive evaluation, a brain MRI, and ^{18}F-Florzolotau PET scans.

SUBJECTS

A total of 55 participants, including 23 normal controls (NCs) and 32 patients with PSP, were recruited for this study. The diagnosis of PSP and its clinical phenotypes were based on the International Parkinson and Movement Disorder Society criteria for the diagnosis of PSP.[2] Neuropsychological assessments were performed for all participants using the Mini-Mental State Examination (MMSE).[17] Disease severity was measured by the Unified Parkinson's Disease Rating Scale (UPDRS) (range, 0–199) and the PSP rating scale (PSPRS) (range, 0–100).[18,19] Patients were asked to discontinue medication before the clinical rating and imaging. The NCs in the study had to be 20 to 80 years old with normal cognitive function (MMSE: 26–30; normal ^{18}F-Florzolotau PET result).

Image Acquisition

^{18}F-Florzolotau was prepared and synthesized at the cyclotron facility of Chang Gung Memorial Hospital.[20] All participants were studied with a Biograph mCT PET/CT system (Siemens Medical Solutions, Malvern, PA) and an integrated PET/MR system (Siemens Biograph mMR scanner). The scanning times for all participants were between 15 and 16 minutes. For the ^{18}F-Florzolotau PET study, a 10-minute scan was acquired 90 minutes after an injection of 185 ± 74 MBq of ^{18}F-Florzolotau. PET images were reconstructed based on the software version VB20 provided by the manufacturer. The reconstructed images had a matrix size of 400 × 400 × 148 and a voxel size of 0.68 × 0.68 × 1.5 mm^3. The MRI protocol has been reported previously.[15] Briefly, it included a sagittal fluid attenuation inversion recovery sequence, whole-brain axial 3-dimensional T1-weighted magnetization-prepared rapid acquisition gradient echo sequence, and whole-head diffusion study. Participants with significant MRI abnormalities were excluded from the study. The diffusion tensor image sequence was acquired along 64 gradient directions for b = 1000 s/mm^2 with an echo planar imaging sequence, and one b = 0 s/mm^2 image was acquired with the diffusion-weighted imaging (DWI) sequence.

Image Analysis

For each participant, we registered ^{18}F-Florzolotau images to individual T1-weighted MRI scans using the SPM12 toolbox.[21] This procedure ensured that each PET image was in alignment with the native MRI scans. The Muller-Gartner method was used for partial volume correction.[22] Then, the high-resolution T1-weighted MRI scans in native space were normalized to the Montreal Neurological Institute (MNI) standard space using the Computational Anatomy Toolbox.[23] This transform matrix was applied to the PET images. For all ^{18}F-Florzolotau images, a traditional cerebellar gray matter (GM) as the reference region and a technique known as parametric estimation of reference signal intensity (PERSI) (Supplementary Fig. S1, http://links.lww.com/CNM/A462), which is used to perform count normalization by using the cerebrum white matter as the reference region, were implemented to compare the diagnostic discriminations between PSP patients and NCs.[5,24] The cortical regions of interest (ROIs) included the bilateral frontal, parietal, temporal, occipital lobes, anterior and posterior cingulate gyri, precuneus, hippocampus, parahippocampus, and sensorimotor cortex, and the subcortical ROIs included the bilateral caudate nucleus, anterior and posterior putamen, globus pallidum, thalamus, midbrain, red nucleus, raphe nucleus, and dentate nucleus. These regions were selected based on the Harvard-Oxford cortical-subcortical structural atlas.[25,26] The average values from both sides were used for subsequent analysis, and 2 meta-ROIs (cortical and subcortical meta-ROIs) were created from all cortical and subcortical ROIs. Finally, the regional SUV ratios (SUVRs) from ^{18}F-Florzolotau PET images were calculated by using the mean intensity in the target ROIs divided by the averaged intensity of the reference regions.

Diffusion MRI data analysis was performed by using ExploreDTI to study the glymphatic activity.[27] The DWI datasets were coregistered to native T1-weighted images. Then, the resulting DWI data were fitted to the DTI model.[28] A fractional anisotropy map of each participant was coregistered to the fractional anisotropy map template of the International Consortium of Brain Mapping (ICBM) DTI-81 Atlas in MNI space, and the accuracy of coregistration was visually confirmed. The ICBM DTI-81 Atlas had labels of the projection (superior and posterior corona radiata) and association (superior longitudinal fasciculus) fibers in the periventricular area. We extracted the periventricular projection and association fibers within the 25 mm to 33 mm range above the anterior-posterior commissure line in MNI space, where the *x* axis line corresponded to the passing direction of the vessels in the deep white matter. Diffusion tensor image analysis along the perivascular space (DTI-ALPS) index and diffusivity from projection and association fibers derived from the ICBM DTI-81 Atlas were calculated as Taoka et al[29] described. A higher DTI-ALPS index represented better glymphatic activity.[30] Brainstem volumes were calculated using FreeSurfer v7.4.0, and the midbrain and pons volumes were calculated using T1-weighted images.[31] Voxel-based morphometry (VBM) analyses were performed using each participant's modulated normalized GM tissue images smoothed with an 8 × 8 × 8-mm isotropic Gaussian kernel as input. The SUVRs of the cortical and subcortical meta-ROIs from ^{18}F-Florzolotau PET images were used as covariates to explore the significantly correlated GM volume in whole-brain regions; the estimated total intracranial volumes were used as covariates to correct for different brain sizes by the multiple regression module in the Computational Anatomy Toolbox.[23]

Statistical Analyses

All statistical analyses were performed using SPSS (version 21.0, Chicago, IL). Continuous variables are expressed as the median ± interquartile range (IQR). Nonparametric Mann-Whitney *U* tests and χ^2/Fisher exact tests were performed to compare data for PSP patients and NCs whenever appropriate. The between-group differences in the regional SUVR values from the ^{18}F-Florzolotau PET images were corrected for multiple comparisons using the

© 2024 The Author(s). Published by Wolters Kluwer Health, Inc.

Downloaded from http://journals.lww.com/nuclearmed by BhDMf5ePHKav1zEoum1tQfN4a+kJLhEZgbsIHo4XMi0hCywCX1AWnYQp/IlQrHD3i3D0OdRyi7TvSFl4Cf3VC4/OAVpDDa8K2+Ya6H515kE= on 04/11/2024

Benjamini-Hochberg procedure, and the significance level was defined as a P value less than 0.05. Regression analyses of the associations between the DTI-ALPS indexes and mean regional SUVR values in the PET images and cognition were performed. In the VBM analyses, the GM volumes that were significantly correlated with SUVRs from the cortical and subcortical meta-ROIs were identified based on a voxel-level height threshold of false discovery rate $P < 0.05$ (false discovery rate corrected) and a cluster-extent threshold of $k > 64$ voxels (64 mm^3).

We used mediation analysis to explore the significance of the regional SUVRs in PET images as a mediator between the DTI-ALPS indexes and PSPRS total scores. Mediation analysis is a statistical model used to quantify a mediating variable in the causal sequence by which an antecedent variable affects a dependent variable[32] and was performed using the PROCESS macro for SPSS (model 4) with a level of confidence at 95% and 5000 bootstrap samples.[33] The mediation analysis was composed of total, direct, and indirect effects. The percent of mediation (Pm) calculated by the indirect effect divided by the total effect was calculated to study the weight of the DTI-ALPS index in the total effect. Statistical significance was defined as a P value less than 0.05.

RESULTS

Demographic Data

Table 1 shows the demographic data of 32 patients with PSP and 23 NCs. PSP phenotypes included PSP–Richardson syndrome (n = 5), PSP-PGF (n = 15), and other phenotypes (n = 12). The mean age of the patients with PSP was not significantly different from that of the NCs (median age of patients with PSP: 68.5 years, IQR: 62.3–72; median age of NCs: 65 years, IQR: 57–71; $P = 0.10$). No significant group differences were found for sex and years of education ($P = 0.30$ and $P = 0.58$, respectively). However, significantly lower MMSE scores, UPDRS total scores, and PSPRS total scores were found in patients with PSP than in NCs (all P's < 0.01). The SUVRs of the cortical and subcortical meta-ROIs from ^{18}F-Florzolotau using PERSI as a reference showed significant differences between patients with PSP and NCs ($P < 0.01$ and $P < 0.01$, respectively). In contrast, using cerebellar GM as a reference, only the SUVRs of the subcortical meta-ROIs significantly differed ($P < 0.01$). In the MRI analysis, the GM volume and midbrain volume but not the pons volume showed significantly lower values in patients with PSP than in NCs ($P = 0.01$, $P = 0.02$, and $P = 0.21$, respectively). The glymphatic activity that was measured by the DTI-ALPS index significantly differed between patients with PSP and NCs ($P = 0.03$).

Comparison of Different Referential Methods in Distinguishing PSP From NCs

We compared the between-group differences in the SUVR values from the cortical and subcortical regions using the cerebellar GM as a reference and the PERSI as a reference. Table 2 shows that no significant between-group differences were found in any of the cortical regions when cerebellar GM was used as the reference. However, the frontal, parietal, occipital, posterior cingulate, precuneus, and sensorimotor cortices showed significant group differences in PERSI as a reference, even after adjusting for multiple comparisons (all P's < 0.05). In the subcortical region analyses, both reference methods

TABLE 1. Demographic Data of Patients With PSP and NCs

	NC (n = 23)	PSP (n = 32)	P*
Demographics			
Age, median (IQR), y	65 (57–71)	68.5 (62.3–72)	0.10
Gender (M:F)	9:14	17:15	0.30
Education, median (IQR), y	12 (9–15)	12 (9–16)	0.58
Clinical history and subtypes			
PSPRS-history, median (IQR)	0 (0–0)	7 (4–9.75)	<0.01
PSPRS-mentation, median (IQR)	0 (0–0)	0 (0–3)	<0.01
PSPRS-bulbar, median (IQR)	0 (0–0)	3 (1.25–4)	<0.01
PSPRS-ocular motor, median (IQR)	0 (0–0)	3 (1–6)	<0.01
PSPRS-limb motor, median (IQR)	0 (0–0)	2 (1–4)	<0.01
PSPRS-gait midline, median (IQR)	0 (0–0)	11.5 (8–13.75)	<0.01
Clinical assessments			
PSPRS total scores, median (IQR)	0 (0–0)	42.5 (20–55.5)	<0.01
UPDRS total scores, median (IQR)	0 (0–0)	40 (27.75–68.25)	<0.01
UPDRS-III scores, median (IQR)	0 (0–0)	21 (14–40)	<0.01
MMSE, median (IQR)	29 (27–30)	27 (21–28.75)	<0.01
PET parameters			
SUVRs in cortical meta-ROI, median (IQR)	0.89 (0.81–0.97)	0.98 (0.89–1.09)	<0.01
SUVRs in subcortical meta-ROI, median (IQR)	1.08 (1.04–1.19)	1.31 (1.18–1.43)	<0.01
MRI parameters			
GM volume, median (IQR), mL	550.46 (519.55–584.06)	520.42 (476.82–570.18)	0.01
Midbrain volume, median (IQR), mL	5.28 (5.09–5.76)	4.99 (4.48–5.59)	0.02
Pons volume, median (IQR), mL	13.62 (12.16–14.23)	12.67 (11.78–14.09)	0.21
DTI-ALPS index, median (IQR)	1.46 (1.27–1.58)	1.29 (1.24–1.39)	0.03

PET parameters were used as a PERSI reference.

*P value: nonparametric Mann-Whitney U tests were used to estimate between-group differences.

© 2024 The Author(s). Published by Wolters Kluwer Health, Inc.

TABLE 2. Comparisons of SUVR From ^{18}F-Florzolotau Tau PET Images Between Patients With PSP and NCs in Cortical and Subcortical Regions Using Cerebellar Gray Matter as a Reference and PERSI as a Reference

	Cerebellar Gray Matter as Reference			PERSI as Reference		
	NC (n = 23)	PSP (n = 32)	*P**	NC (n = 23)	PSP (n = 32)	*P**
Cortical regions						
Frontal lobe	0.81 (0.75–0.94)	0.85 (0.74–0.93)	0.81	0.84 (0.76–0.91)	0.89 (0.84–0.99)	<0.05
Parietal lobe	0.81 (0.79–0.94)	0.90 (0.79–0.99)	0.48	0.85 (0.77–0.94)	0.96 (0.88–1.08)	<0.05
Temporal lobe	0.96 (0.91–1.05)	0.98 (0.85–1.09)	0.81	0.98 (0.89–1.04)	1.07 (0.95–1.14)	0.07
Occipital lobe	0.87 (0.83–0.98)	0.96 (0.88–1.01)	0.13	0.89 (0.81–0.98)	1.04 (0.94–1.11)	<0.05
Hippocampus gyrus	1.19 (0.99–1.87)	1.19 (0.86–1.65)	0.46	1.28 (0.96–1.77)	1.17 (0.90–1.82)	0.40
Parahippocampus gyrus	0.92 (0.87–0.99)	0.93 (0.86–1.04)	0.81	0.92 (0.87–0.99)	0.93 (0.86–1.04)	0.66
Anterior cingulate gyrus	0.88 (0.82–0.95)	0.88 (0.86–1.01)	0.81	0.89 (0.82–0.94)	0.94 (0.87–1.01)	0.13
Posterior cingulate gyrus	0.95 (0.86–0.99)	0.92 (0.91–1.34)	1.00	0.92 (0.87–1.01)	1.02 (0.89–1.19)	<0.05
Precuneus	0.91 (0.88–0.97)	0.91 (0.86–1.04)	0.81	0.91 (0.84–1.04)	1.01 (0.91–1.20)	<0.05
Sensorimotor cortex	0.81 (0.75–0.92)	0.88 (0.82–0.97)	0.10	0.83 (0.75–0.89)	0.93 (0.89–1.02)	<0.05
Subcortical regions						
Caudate nucleus	0.65 (0.58–0.74)	0.60 (0.55–0.74)	0.62	0.66 (0.55–0.75)	0.68 (0.61–0.75)	0.32
Anterior putamen	1.03 (0.96–1.11)	1.24 (1.05–1.39)	<0.05	1.00 (0.95–1.10)	1.26 (1.21–1.35)	<0.05
Posterior putamen	1.05 (0.94–1.13)	1.20 (1.06–1.37)	<0.05	1.01 (0.94–1.11)	1.30 (1.19–1.41)	<0.05
Globus pallidum	1.24 (1.11–1.29)	1.42 (1.29–1.64)	<0.05	1.19 (1.13–1.24)	1.55 (1.43–1.78)	<0.05
Thalamus	1.32 (1.09–1.61)	1.37 (1.21–1.52)	0.81	1.33 (1.04–1.55)	1.45 (1.22–1.68)	0.32
Midbrain	0.97 (0.90–1.02)	1.21 (0.98–1.32)	<0.05	0.98 (0.89–1.04)	1.19 (1.08–1.40)	<0.05
Red nucleus	1.27 (1.18–1.35)	1.45 (1.32–1.74)	<0.05	1.20 (1.15–1.35)	1.57 (1.43–1.91)	<0.05
Raphe nucleus	1.11 (1.00–1.16)	1.54 (1.15–1.70)	<0.05	1.11 (0.97–1.18)	1.49 (1.29–1.86)	<0.05
Dentate nucleus	1.36 (1.27–1.43)	1.39 (1.19–1.52)	0.81	1.29 (1.24–1.48)	1.41 (1.31–1.65)	0.05

**P* value: nonparametric Mann-Whitney *U* tests were used to estimate between-group differences related to semiquantitative PET parameters in different regions; in all analyses, the Benjamini-Hochberg procedure was applied to correct for multiple comparisons.

Downloaded from http://journals.lww.com/nuclearmed by BhDMf5ePHKav1zEoum1tQfN4a+kJLhEZgbsIHo4XMi0hCywCX1AWnYQp/IlQrHD3i3D0OdRyi7TvSFl4Cf3VC4/OAVpDDa8K2+Ya6H515kE= on 04/11/2024

showed significant between-group differences in the anterior and posterior putamen, globus pallidum, midbrain, red nucleus, and raphe nucleus regions after adjusting for multiple comparisons (all *P*'s < 0.05). In addition, the dentate nucleus showed borderline significance in the between-group differences with PERSI as a reference ($P = 0.047$). Using PERSI as a reference, the SUVRs from the cortical and subcortical meta-ROIs showed significantly positive correlations with the PSPRS total scores, UPDRS total scores, and UPDRS-III scores (all *P*'s < 0.01) (Figs. 1A, B). For MMSE scores, significantly negative correlations were found between the SUVRs from the cortical meta-ROIs and subcortical meta-ROIs ($P < 0.01$ and $P = 0.04$, respectively). In contrast, using cerebellar GM as a reference, neither the subcortical nor cortical meta-ROIs showed significant associations with the PSPRS total scores, UPDRS total scores, UPDRS-III scores, or MMSE scores (all *P*'s > 0.05). Based on these findings, the associations between the SUVR values from the regional ^{18}F-Florzolotau PET images and clinical parameters were analyzed using PERSI as a reference.

Associations of Cortical and Subcortical Tau Burden With Clinical, GM Volume, and Glymphatic Activity

We used the upper 1.5 standard deviation as a cutoff value (SUVR = 1.04) in the cortical meta-ROIs from NCs to separate patients with PSP into a cortical involvement group (n = 11) and a noncortical involvement group (n = 21). Figure 2A shows the significantly higher SUVRs in the parietal, temporal, and occipital lobes in the cortical involvement group of PSP patients. Table 3 shows the comparison of the clinical measures, DTI-ALPS indexes, and brain volumes in patients with PSP according to the cortical and noncortical involvement groups. Significantly higher PSPRS total scores, UPDRS total scores, and UPDRS-III scores were found in

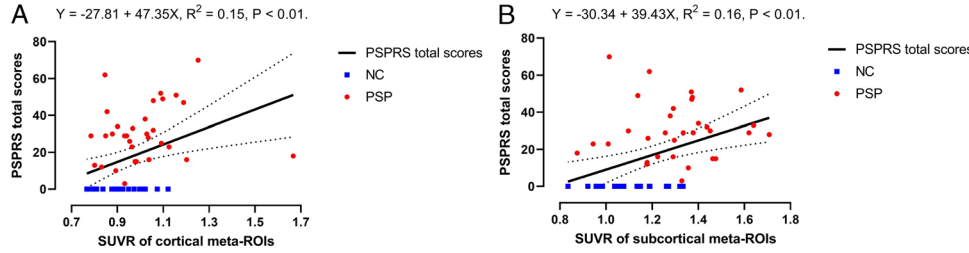

FIGURE 1. Tau deposition in the cortical and subcortical meta-ROIs is associated with the PSPRS total scores, DTI-ALPS indexes, GM atrophy, and midbrain volumes using the PERSI reference. **A**, Tau deposition in the cortical meta-ROIs showed a significantly positive correlation with the PSPRS total scores. **B**, Tau deposition in the subcortical meta-ROIs showed a significantly positive correlation with the PSPRS total scores.

© 2024 The Author(s). Published by Wolters Kluwer Health, Inc.

the cortical involvement group than in the noncortical involvement group ($P = 0.04$, 0.02, and <0.01, respectively). However, there was no significant between-group difference in terms of MMSE scores. The cortical involvement group had significantly higher SUVRs of ^{18}F-Florzolotau images from the cortical meta-ROIs than the noncortical involvement group ($P < 0.01$). However, the SUVRs from the subcortical meta-ROIs did not show a significant difference between the groups ($P = 0.39$).

The Associations Among Regional Tau Depositions, Glymphatic Activity, and GM Volumes

Pearson's correlation coefficients were used to evaluate associations of the SUVRs from the cortical and subcortical meta-ROIs with the clinical parameters (PSPRS total scores, UPDRS total scores, and MMSE scores) (Fig. 3A). The SUVRs from the cortical and subcortical meta-ROIs showed significant associations with clinical parameters (PSPRS total scores, UPDRS total scores, and MMSE scores). In the regional analysis, the SUVRs from the cortical regions (eg, frontal, parietal, occipital lobes, anterior and posterior cingulate gyri, precuneus, and sensorimotor cortex) and subcortical regions (eg, anterior and posterior putamen, globus pallidum, midbrain, red nucleus, and raphe nucleus) showed significantly positive correlations with the PSPRS total scores even after adjusting for age, sex, and years of education as covariates (all P's < 0.05). With regard to the MMSE scores, the SUVRs from the cortical regions (eg, frontal, parietal, temporal lobes, anterior and posterior cingulate gyri, precuneus, and sensorimotor cortex) and subcortical regions (eg, caudate nucleus, anterior and posterior putamen, and raphe nucleus) showed significantly negative correlations even after adjustment for age, sex, and years of education (all P's < 0.05).

Downloaded from http://journals.lww.com/nuclearmed by BhDMf5ePHKav1zEoum1tQfN4a+kJLhEZgbsIHo4XMi0hCywCX1AWnYQp/IlQrHD3i3D0OdRyi7TvSFl4Cf3VC4/OAVpDDa8K2+Ya6H515kE= on 04/11/2024

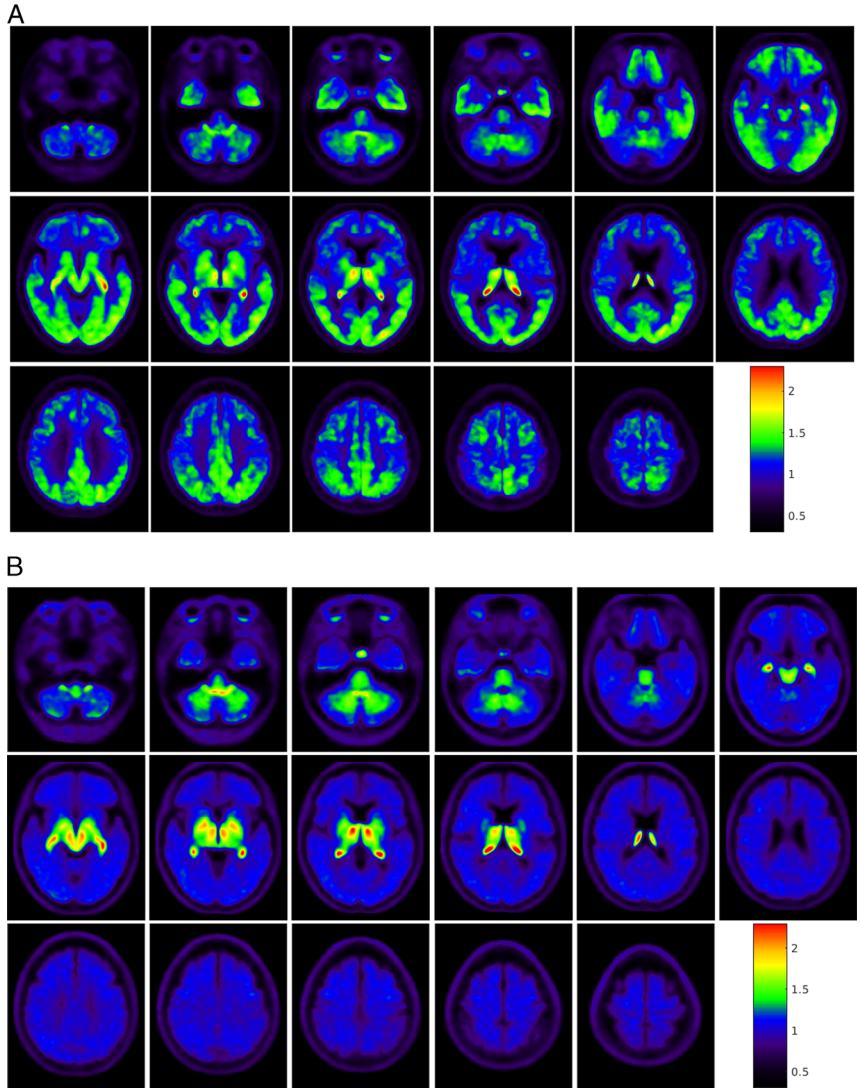

FIGURE 2. Schematic showing the averaged images from the cortical involvement group (**A**, n = 11) and the noncortical involvement group (**B**, n = 21) of patients with PSP after partial volume correction; the group assignment was based on the cutoff value (SUVR = 1.04) in the cortical meta-ROIs. **A**, In the cortical involvement group, significantly higher tau deposition was observed in the parietal, temporal, and occipital lobes as well as in the basal ganglia. **B**, In the noncortical involvement group, only the putamen, globus pallidum, midbrain, red nucleus, and raphe nucleus regions showed tau deposition. The color bar represents the corresponding SUVR values.

© 2024 The Author(s). Published by Wolters Kluwer Health, Inc.

TABLE 3. Comparisons of Clinical Parameters, DTI-ALPS Indexes, and Brain Volumes in Patients With PSP According to the Cortical and Noncortical Involvement of Tau Deposition Using the PERSI Reference

	Cortical Involvement Group (n = 11)	Noncortical Involvement Group (n = 21)	*P**
Demographics			
Age, median (IQR), y	72 (67–73)	67 (61–71)	0.07
Gender (M:F)	5:6	12:9	0.53
Education, median (IQR), y	12 (6–16)	12 (9–16)	0.70
Clinical assessments			
PSPRS total scores, median (IQR)	47 (23–51)	29 (15–31.5)	0.04
UPDRS total scores, median (IQR)	71 (38–87)	39 (25–46)	0.02
UPDRS-III scores, median (IQR)	41 (18–54)	15 (12–25)	<0.01
MMSE, median (IQR)	21 (10–29)	27 (22.5–28.5)	0.19
PET parameters			
SUVRs in cortical meta-ROI, median (IQR)	1.12 (1.09–1.20)	0.93 (0.85–0.98)	<0.01
SUVRs in subcortical meta-ROI, median (IQR)	1.29 (1.01–1.38)	1.33 (1.19–1.46)	0.39
MRI parameters			
GM volumes, median (IQR), mL	514.07 (447.27–572.11)	520.59 (494.21–550.37)	0.54
Midbrain volume, median (IQR), mL	5.24 (4.33–5.62)	4.79 (4.49–5.57)	0.77
Pons volume, median (IQR), mL	13.35 (10.28–14.45)	12.28 (11.78–13.68)	0.54
DTI-ALPS index, median (IQR)	1.31 (1.22–1.39)	1.29 (1.24–1.37)	0.79

**P* value: nonparametric Mann-Whitney *U* tests were used to estimate between-group differences.

Downloaded from http://journals.lww.com/nuclearmed by BhDMf5ePHKav1zEoum1tQfN4a+kJLhEZgbsIHo4XMi0hCywCX1AWnYQp/IlQrHD3i3D0OdRyi7TvSFl4Cf3VC4/OAVpDDa8K2+Ya6H515kE= on 04/11/2024

In the VBM analyses, the SUVRs from the cortical meta-ROIs showed significantly negative correlations with the GM volumes in the bilateral parietal, temporal, medial frontal, and anterior cingulate regions (Fig. 3B). No significant correlation was found between the SUVRs from the subcortical meta-ROIs and GM volumes.

In DTI-ALPS index analysis, the SUVRs from the cortical but not the subcortical meta-ROIs showed a significantly negative correlation ($P = 0.03$ and $P = 0.07$, respectively) (Fig. 3C). In the regional analysis, the SUVRs from the parietal, temporal, and occipital lobes showed significantly negative correlations with the DTI-ALPS indexes ($P = 0.03$, $P = 0.03$, and $P = 0.04$, respectively). In the midbrain volume analysis, the SUVRs from the subcortical but not cortical meta-ROIs showed a significantly negative correlation with midbrain volumes ($P = 0.01$ and $P = 0.63$, respectively) (Fig. 3D). In the regional analysis, the SUVRs from the anterior and posterior putamen, globus pallidum, midbrain, red nucleus, raphe nucleus, and dentate nucleus showed significantly negative correlations with the midbrain volumes (all P's < 0.05).

The Associations Between MRI Parameters and Clinical Parameters

The midbrain volume showed a significantly negative correlation with the PSPRS total scores ($P < 0.01$) (Fig. 3E). The DTI-ALPS indexes showed a significantly negative correlation with the PSPRS total scores but not the MMSE scores ($P = 0.01$ and $P = 0.22$, respectively) (Fig. 3F).

Mediation Analysis Among Glymphatic Dysfunction, Tau Depositions, and Clinical Parameters

Finally, we examined the contribution of cortical and subcortical tau deposition between the DTI-ALPS indexes and PSPRS total scores. Using the mediation analysis, the SUVRs of the ^{18}F-Florzolotau PET images from the cortical meta-ROIs showed significant total and indirect mediation effects between the DTI-ALPS indexes and PSPRS total scores (Pm = 27.04%; total effect B = −37.29, $P = 0.01$; direct effect B = −27.21, $P = 0.07$; indirect effect B = −10.08, 95% confidence interval [CI] = −25.35 to −0.71). When we further included midbrain volume as a covariate in the model, the cortical meta-ROIs still had significant total and indirect mediation effects (Pm = 43.52%; total effect B = −29.37, $P = 0.03$; direct effect B = −16.59, $P = 0.19$; indirect effect B = −12.78, 95% CI = −26.07 to −2.58) (Fig. 4A). In the regional analysis, there was a significant full mediation effect of the SUVRs in the parietal region between the DTI-ALPS index and PSPRS total scores even after adjusting for midbrain volume (Pm = 46.75%; total effect B = −29.37, $P = 0.03$; direct effect B = −15.64, $P = 0.22$; indirect effect B = −13.73, 95% CI = −28.16 to −3.43). In addition, there was a significant full mediation effect of the SUVRs in the occipital region between the DTI-ALPS index and PSPRS total scores even after adjusting for midbrain volume (Pm = 36.35%; total effect B = −29.37, $P = 0.03$; direct effect B = −18.69, $P = 0.16$; indirect effect B = −10.68, 95% CI = −23.66 to −4.02) (Figs. 4B–D). On the other hand, the SUVRs from the subcortical meta-ROIs did not show a significant mediation effect between the DTI-ALPS indexes and PSPRS total scores (total effect B = 37.29, $P = 0.01$ direct effect B = −27.95, $P = 0.05$; indirect effect B = −9.34, 95% CI = −22.62 to 0.30). Because the DTI-ALPS indexes did not show a significant association with the MMSE scores, the SUVRs from the cortical and subcortical meta-ROIs did not show significant mediation effects between the DTI-ALPS indexes and MMSE scores.

DISCUSSION

This study investigated the role of tau protein deposition in the cortical and subcortical regions among glymphatic dysfunction, GM atrophy, and clinical manifestations in patients with PSP and NCs. We used regional SUVRs from ^{18}F-Florzolotau PET images to characterize the burden of tau deposition. Our study suggested that tau deposition in the cortical and subcortical regions had different clinical significance and that cortical tau deposition is a significant mediator between glymphatic dysfunction and disease severity in patients with PSP. Our results provide evidence for glymphatic dysfunction in the pathogenesis of PSP.

© 2024 The Author(s). Published by Wolters Kluwer Health, Inc.

Downloaded from http://journals.lww.com/nuclearmed by BhDMf5ePHKav1zEoum1tQfN4a+kJLhEZgbsIHo4XMi0hCywCX1AWnYQp/IlQrHD3i3D0OdRyi7TvSFl4Cf3VC4/OAVpDDa8K2+Ya6H515kE= on 04/11/2024

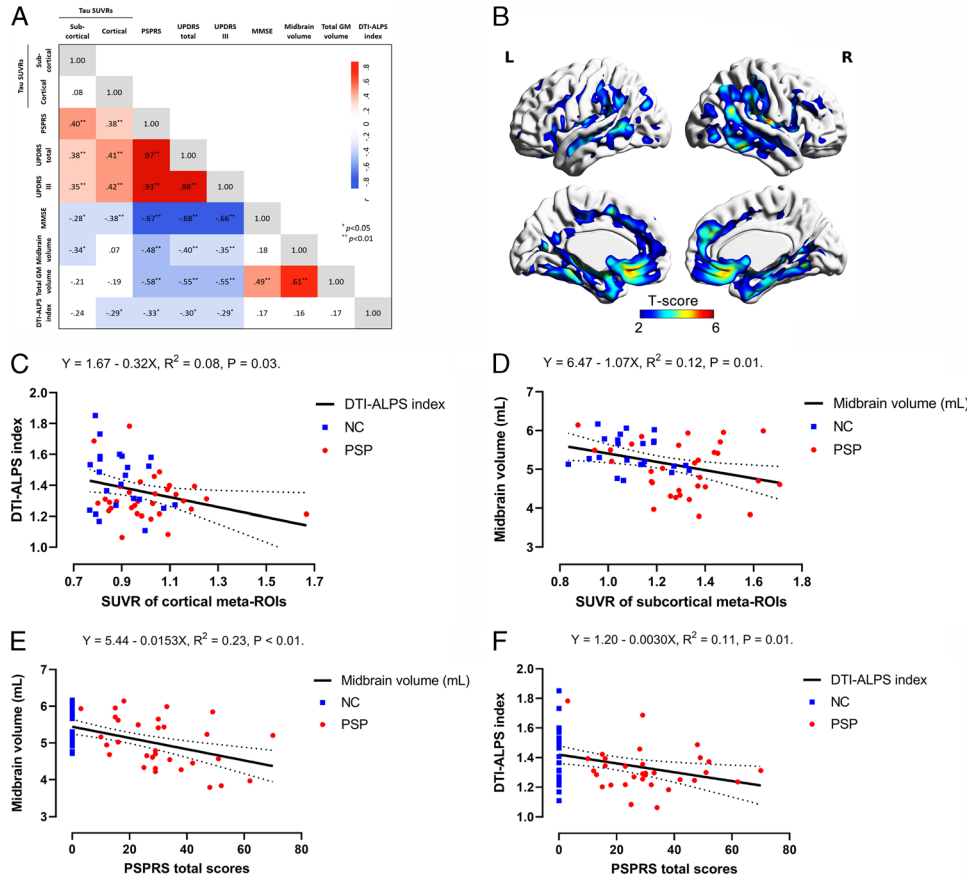

FIGURE 3. Tau deposition in the cortical and subcortical meta-ROIs is associated with the PSPRS total scores, DTI-ALPS indexes, GM atrophy, and midbrain volumes. **A**, The heatmap shows Pearson correlation matrix of tau depositions, clinical assessments, and MRI parameters. **B**, Three-dimensional render views show that tau deposition in the cortical meta-ROIs has significantly negative correlations with the GM volumes in the medial frontal, parietal, and temporal regions. The color bar indicates the significance of the associations. **C**, Tau deposition in the cortical meta-ROIs shows a significantly negative correlation with the DTI-ALPS indexes. **D**, Tau deposition in the subcortical meta-ROIs shows a significantly negative correlation with the midbrain volumes. **E**–**F**, The PSPRS total scores show significantly negative correlations with the midbrain volumes (**E**) and DTI-ALPS indexes (**F**).

Glymphatic Dysfunction in PSP

Many studies have found glymphatic dysfunction in synucleinopathy, tauopathy, amyloidopathy, and TDP-43 deposition.[15,34–36] In movement disorders, several studies have demonstrated that glymphatic dysfunction contributes to the pathogenesis and progression of PD but is relatively rare in PSP.[37,38] Since the glymphatic system could be a potential target for pharmacological or nonpharmacological intervention in neurodegenerative diseases, it is important to unravel the hidden information behind the surrogate markers for glymphatic activity.[39,40] However, glymphatic research in humans is very difficult due to the invasive methodology; therefore, most studies use indirect indicators, such as the DTI-ALPS index or perivascular space.[41] As a limitation of the technique, the DTI-ALPS index was evaluated using the whole-brain glymphatic activity rather than the regional activity.

In our study, we found that tau depositions were involved in the mediation effect between the DTI-ALPS index and PSPRS scores, implying that the glymphatic system may be responsible for the severity of PSP. In addition, when considering the effects of tau distribution, the influence of glymphatic dysfunction on PSP clinical symptoms is significantly affected by the cortical tau burden. Furthermore, the full mediation effect of tau depositions in the parietal and occipital regions between the DTI-ALPS indexes and PSPRS total scores suggested that this association was strongly mediated by regional tau depositions. Our results provide a possible explanation for the worsening of clinical symptoms in patients with PSP. In light of the final common pathway hypothesis based on previous animal and human studies of AD, glymphatic dysfunction becomes an unrevealing pathway of pathological protein-derived neurodegenerative diseases, and certain cortical regions are specifically crucial in determining the disease severity of PSP.[10,14,36] Glymphatic dysfunction may be involved in different phenotypes of PSP. Parkinson disease is another typical subcortical neurodegenerative disease, and although the associations between the DTI-ALPS index and clinical parameters have been extensively studied, the contribution of pathological proteins in the cortical and subcortical regions to the glymphatic system still needs further investigation.[12,42]

An alternative explanation for the cortical tau burden in the mediation analysis could be that the clearance of subcortical tau deposition was drainage from another pathway, which could not be detected by the DTI-ALPS index. Animal studies have identified at least a dorsal and ventral part of the lymphatic drainage system.[43,44]

© 2024 The Author(s). Published by Wolters Kluwer Health, Inc.

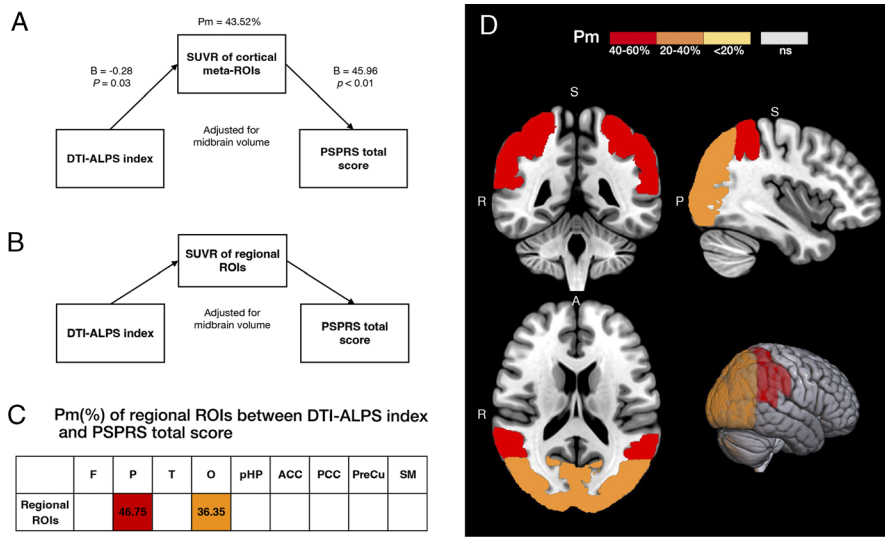

FIGURE 4. Schematic of the mediation analysis showing tau deposition in the cortical meta-ROIs (**A**) and regional ROIs (**B**) as significant mediators after correction for midbrain volume. **A**, Tau deposition in the cortical meta-ROIs is a statistically significant full mediator of the relationship between the DTI-ALPS indexes and PSPRS total scores. **B**, Schematic showing the regional ROI analysis. **C**, The percentage of mediation (Pm) analysis of regional tau deposition between the DTI-ALPS indexes and PSPRS total scores after correction for the midbrain volume from the indirect mediation analysis. **D**, Significant regions are shown in the different colored bars. Nonsignificant regions are shown in white. Background regions are shown in gray. F, frontal; P, parietal; T, temporal; O, occipital; pHP, parahippocampus; ACC, anterior cingulate cortex; PCC, posterior cingulate cortex; PreCu, precuneus; SM, sensorimotor cortex.

Downloaded from http://journals.lww.com/nuclearmed by BhDMf5ePHKav1zEoum1tQfN4a+kJLhEZgbsIHo4XMi0hCywCX1AWnYQp/IlQrHD3i3D0OdRyi7TvSFl4Cf3VC4/OAVpDDa8K2+Ya6H515kE= on 04/11/2024

The possibility of "cortical" and "subcortical" pathways of glymphatic drainage could be raised. A study of normal pressure hydrocephalus in humans demonstrated that the clearance of contrast media by intrathecal injection of gadobutrol had locus differences, with faster clearance in the foramen magnum, sylvian fissure, and pontine cistern than in the precentral sulcus.[45] Since the DTI-ALPS index is derived from diffusion MRI measurements in the cerebral periventricular regions, it is reasonable to assume that subcortical tau deposition was not associated with the DTI-ALPS index, which could be determined by our findings.[29]

Cortical and Subcortical Tau Burden Contributes to Different Features in PSP

Recently, Scotton et al[8] used a machine learning method to explore the patterns of atrophy on MRI scans in patients with PSP. They identified 2 distinct subtypes of spatiotemporal patterns, namely, the "subcortical subtype" and the "cortical subtype." The subcortical subtype was associated with worse PSPRS scores than the cortical subtype. There was no significant difference in MMSE scores between the 2 subtypes.[8] According to the study by Scotton et al,[8] PSP has 2 variants: PSP-cortical variant (PSP-frontal, PSP–speech/language, or PSP-corticobasal) and PSP-subcortical variant (PSP-parkinsonism or PSP-PGF). In our current study, out of 27 patients with PSP variant, 2 had PSP-cortical variant and 25 had PSP-subcortical variant. The Fisher exact test did not reveal any significant difference between the cortical and noncortical involvement groups based on the criteria of tau PET images ($P = 1$). Therefore, our findings do not support the classification of groups based on cortical and noncortical involvement from Tau PET images as reflecting different clinical PSP-variants. Due to the limited number of cases and lack of longitudinal follow-up in our study, we cannot determine whether the progressive subcortical to cortical tau burden simply reflects the natural history of PSP.

Two distinct spatiotemporal patterns with associated clinical features in PSP have been identified in another study using tau PET imaging.[9] They found that tau spread appeared first in the subcortical regions and ultimately in the cortical regions. In our study, the subcortical tau burden demonstrated a significant difference between patients with PSP and NCs. In addition, for tau protein deposition, the cortical involvement group had significantly higher severity of clinical scores than the noncortical involvement group, which indicated that the subcortical tau burden could discriminate patients with PSP from NCs in the early stage of PSP.[5,46] In addition, cortical tau deposition was significantly correlated with the DTI-ALPS index and had a significant mediation effect between the DTI-ALPS index and PSPRS total scores, whereas subcortical tau deposition did not play a significant role with the DTI-ALPS index. The contribution of cortical versus subcortical tau burden to the different associations between the DTI-ALPS index and PSPRS total scores has not been previously reported.

Reference Regions of Tau PET Images in Patients With PSP

The recent development of second-generation tau PET tracers has enabled the visualization of in vivo tau deposition in patients with PSP.[47] Therefore, the selection of a reference region is important because it is assumed that the reference region is free of tau lesions containing binding components, which might contrast with tau accumulation in other regions. In a neuropathology study of PSP, 6 stages of topographical evolution from the subthalamic nucleus, globus pallidus, striatum, cerebellum with the dentate nucleus, to the frontal and occipital cortices have been documented.[1] In the past, tau PET studies in patients with PSP have used the cerebellar GM as the reference region.[4–6,46] However, several methods using the noncerebellar region as a reference have shown significantly improved diagnostic discrimination in patients with AD and non-AD tauopathy.[48,49] In our study, using PERSI as a reference

© 2024 The Author(s). Published by Wolters Kluwer Health, Inc.

revealed more significant tau depositions in the cortical regions than using the cerebellar GM as a reference, even after adjusting for multiple comparisons. In addition, the coefficient of variation in the PERSI method was smaller than that in the cerebellar GM as a reference (19% vs 24%). Furthermore, tau depositions in cortical and subcortical ROIs showed significant associations with clinical parameters when using PERSI as a reference but not when the cerebellar GM was used as a reference. Although several more sophisticated reference methods have been proposed for the quantification of tau deposition in diverse neurodegenerative disorders by ^{18}F-Florzolotau PET, our study revealed that using cerebellar GM as a reference could mask tau deposition in many cortical regions.[50,51] In partial volume correction, the significant GM atrophy in patients with PSP justified the need for the procedure. We still performed a nonpartial volume correction analysis, and the results showed a similar trend with partial volume correction results as reported in previous studies.[52,53]

LIMITATIONS

Several limitations need to be addressed in the current study. First, the correlation of the DTI-ALPS index with human glymphatic function has not yet been validated by pathophysiological studies. There has been only one study that directly compared glymphatic activity measurement between the intrathecal contrast media administration method and the DTI-ALPS index method.[30] Recently, several methods have been developed that may reveal regional glymphatic activity.[54–56] Therefore, the relationship between the DTI-ALPS index and glycemic clearance should be interpreted with caution. The sequential effect among glymphatic dysfunction, tau deposition, and clinical symptoms needs to be verified in longitudinal studies. Second, our study was a small, single-center, cross-sectional study, and we could not investigate the association between ^{18}F-Florzolotau imaging results and postmortem findings. We could not determine whether cortical tau deposition can exist in the absence of subcortical tau burden in our PSP study. The amyloid and alpha-synuclein biomarkers were also unavailable in our study, and we could not estimate the contributions of these copathologies. Third, we acknowledge that our investigation included tau deposition from subcortical regions combined with/without cortical regions in patients with PSP. Consequently, it would be inappropriate to definitively deduce from our findings that the DTI-ALPS index is entirely unrelated to subcortical tau depositions. To further elucidate this matter, it would be advantageous to recruit individuals with PSP in the earliest stages of the condition and whose condition is devoid of any cortical involvement. Finally, the different variants of PSP and their associations with tau deposition and glymphatic activity could not be determined because of the limited number of cases, which may contribute to the lack of a significant difference in the DTI-ALPS index between the cortical and noncortical involvement groups. In addition, we did not find an association between cognition and glymphatic activity, which may be related to our assessment tool.[57] Nevertheless, our study revealed that both cortical and subcortical tau burden contribute to the various clinical features and may explain the worsening of PSP and its variants through glymphatic dysfunction.

CONCLUSIONS

In patients with PSP, second-generation tau PET imaging showed increased tau deposition in both the cortical and subcortical regions, which is significantly associated with clinical measures. Tau deposition in the parietal and occipital lobes plays an important role in glymphatic dysfunction and disease severity. The association between the DTI-ALPS index and regional proteinopathy needs to be evaluated in the future.

Downloaded from http://journals.lww.com/nuclearmed by BhDMf5ePHKav1zEoum1tQfN4a+kJLhEZgbsIHo4XMi0hCywCX1AWnYQp/IlQrHD3i3D0OdRyi7TvSFl4Cf3VC4/OAVpDDa8K2+Ya6H515kE= on 04/11/2024

ACKNOWLEDGMENTS

The authors acknowledge the administrative support of the Chang Gung Memorial Hospital Clinical Trial Center—which is funded by the Taiwanese Ministry of Health and Welfare (grants MOHW111-TDU-B-212-134005, MOHW112-TDU-B-212-144005). This study was financially supported by grants from the Taiwanese Ministry of Health and Welfare (MOHW111-TDU-B-212-134005, MOHW112-TDU-B-212-144005), the National Science and Technology Council (MOST 111-2314-B-182A-036-MY2, 109-2314-B-182A-043-MY3, 112-2623-E-182A-001-NU), and the Chang Gung Memorial Hospital Research Fund (CMRPVVL0281). The precursors used in the synthesis of ^{18}F-Florzolotau were generously provided by Aprinoia Therapeutics.

REFERENCES

1. Kovacs GG, Lukic MJ, Irwin DJ, et al. Distribution patterns of tau pathology in progressive supranuclear palsy. *Acta Neuropathol*. 2020;140:99–119.
2. Hoglinger GU, Respondek G, Stamelou M, et al. Clinical diagnosis of progressive supranuclear palsy: the movement disorder society criteria. *Mov Disord*. 2017;32:853–864.
3. Hauw JJ, Daniel SE, Dickson D, et al. Preliminary NINDS neuropathologic criteria for Steele-Richardson-Olszewski syndrome (progressive supranuclear palsy). *Neurology*. 1994;44:2015–2019.
4. Tagai K, Ono M, Kubota M, et al. High-contrast in vivo imaging of tau pathologies in Alzheimer's and non-Alzheimer's disease tauopathies. *Neuron*. 2021;109:42–58.e48.
5. Liu FT, Lu JY, Li XY, et al. (18)F-Florzolotau PET imaging captures the distribution patterns and regional vulnerability of tau pathology in progressive supranuclear palsy. *Eur J Nucl Med Mol Imaging*. 2023;50:1395–1405.
6. Messerschmidt K, Barthel H, Brendel M, et al. (18)F-PI-2620 tau PET improves the imaging diagnosis of progressive supranuclear palsy. *J Nucl Med*. 2022;63:1754–1760.
7. Shah GV. Using MRI to identify supranuclear palsy from Parkinson disease and dementia with Lewy bodies. *Radiology*. 2019;293:654–655.
8. Scotton WJ, Shand C, Todd E, et al. Uncovering spatiotemporal patterns of atrophy in progressive supranuclear palsy using unsupervised machine learning. *Brain Commun*. 2023;5:fcad048.
9. Hong J, Lu J, Liu F, et al. Uncovering distinct progression patterns of tau deposition in progressive supranuclear palsy using [(18)F]Florzolotau PET imaging and subtype/stage inference algorithm. *EBioMedicine*. 2023;97:104835.
10. Nedergaard M, Goldman SA. Glymphatic failure as a final common pathway to dementia. *Science*. 2020;370:50–56.
11. Saito Y, Kamagata K, Andica C, et al. Glymphatic system impairment in corticobasal syndrome: diffusion tensor image analysis along the perivascular space (DTI-ALPS). *Jpn J Radiol*. 2023;41:1226–1235.
12. Shen T, Yue Y, Ba F, et al. Diffusion along perivascular spaces as marker for impairment of glymphatic system in Parkinson's disease. *NPJ Parkinsons Dis*. 2022;8:174.
13. Ota M, Sato N, Takahashi Y, et al. Correlation between the regional brain volume and glymphatic system activity in progressive supranuclear palsy. *Dement Geriatr Cogn Disord*. 2023.
14. Harrison IF, Ismail O, Machhada A, et al. Impaired glymphatic function and clearance of tau in an Alzheimer's disease model. *Brain*. 2020;143:2576–2593.
15. Hsu JL, Wei YC, Toh CH, et al. Magnetic resonance images implicate that glymphatic alterations mediate cognitive dysfunction in Alzheimer disease. *Ann Neurol*. 2023;93:164–174.
16. Zhang Y, Zhang C, He XZ, et al. Interaction between the glymphatic system and alpha-synuclein in Parkinson's disease. *Mol Neurobiol*. 2023;60:2209–2222.
17. Folstein MF, Folstein SE, McHugh PR. "Mini-mental state". A practical method for grading the cognitive state of patients for the clinician. *J Psychiatr Res*. 1975;12:189–198.
18. Hall DA, Stebbins GT, Litvan I, et al. Clinimetric analysis of the motor section of the progressive supranuclear palsy rating scale: reliability and factor analysis. *Mov Disord Clin Pract*. 2016;3:65–67.
19. Goetz CG, Tilley BC, Shaftman SR, et al. Movement Disorder Society–sponsored revision of the Unified Parkinson's Disease Rating Scale (MDS-UPDRS): scale presentation and clinimetric testing results. *Mov Disord*. 2008;23:2129–2170.

© 2024 The Author(s). Published by Wolters Kluwer Health, Inc.

20. Weng CC, Hsiao IT, Yang QF, et al. Characterization of (18)F-PM-PBB3 ((18)F-APN-1607) uptake in the rTg4510 mouse model of Tauopathy. *Molecules*. 2020;25:1750.
21. Ashburner J, Friston KJ. Unified segmentation. *Neuroimage*. 2005;26: 839–851.
22. Gonzalez-Escamilla G, Lange C, Teipel S, et al. PETPVE12: an SPM toolbox for partial volume effects correction in brain PET—application to amyloid imaging with AV45-PET. *Neuroimage*. 2017;147:669–677.
23. Ashburner J, Friston KJ. Diffeomorphic registration using geodesic shooting and Gauss-Newton optimisation. *Neuroimage*. 2011;55:954–967.
24. Southekal S, Devous MD Sr., Kennedy I, et al. Flortaucipir F 18 quantitation using parametric estimation of reference signal intensity. *J Nucl Med*. 2018; 59:944–951.
25. Frazier JA, Chiu S, Breeze JL, et al. Structural brain magnetic resonance imaging of limbic and thalamic volumes in pediatric bipolar disorder. *Am J Psychiatry*. 2005;162:1256–1265.
26. Tziortzi AC, Searle GE, Tzimopoulou S, et al. Imaging dopamine receptors in humans with [^{11}C]-(+)-PHNO: dissection of D3 signal and anatomy. *Neuroimage*. 2011;54:264–277.
27. Leemans AJB, Sijbers J, Jones DK. ExploreDTI: A graphical toolbox for processing, analyzing, and visualizing diffusion MR data. *17th Annual Meeting of Intl Soc Mag Reson Med*. 2009;3537.
28. Basser PJ, Mattiello J, LeBihan D. MR diffusion tensor spectroscopy and imaging. *Biophys J*. 1994;66:259–267.
29. Taoka T, Masutani Y, Kawai H, et al. Evaluation of glymphatic system activity with the diffusion MR technique: diffusion tensor image analysis along the perivascular space (DTI-ALPS) in Alzheimer's disease cases. *Jpn J Radiol*. 2017;35:172–178.
30. Zhang W, Zhou Y, Wang J, et al. Glymphatic clearance function in patients with cerebral small vessel disease. *Neuroimage*. 2021;238:118257.
31. Iglesias JE, Van Leemput K, Bhatt P, et al. Bayesian segmentation of brainstem structures in MRI. *Neuroimage*. 2015;113:184–195.
32. MacKinnon DP, Valente MJ, Gonzalez O. The correspondence between causal and traditional mediation analysis: the link is the mediator by treatment interaction. *Prev Sci*. 2020;21:147–157.
33. Hayes AF. *Introduction to Mediation, Moderation, and Conditional Process Analysis: A Regression-Based Approach*. 2nd ed. New York, NY: Guilford Press; 2018.
34. Bae YJ, Kim JM, Choi BS, et al. Altered brain glymphatic flow at diffusion-tensor MRI in rapid eye movement sleep behavior disorder. *Radiology*. 2023; 307:e221848.
35. Zamani A, Walker AK, Rollo B, et al. Impaired glymphatic function in the early stages of disease in a TDP-43 mouse model of amyotrophic lateral sclerosis. *Transl Neurodegener*. 2022;11:17.
36. Iliff JJ, Wang M, Liao Y, et al. A paravascular pathway facilitates CSF flow through the brain parenchyma and the clearance of interstitial solutes, including amyloid β. *Sci Transl Med*. 2012;4:147ra111.
37. Scott-Massey A, Boag MK, Magnier A, et al. Glymphatic system dysfunction and sleep disturbance may contribute to the pathogenesis and progression of Parkinson's disease. *Int J Mol Sci*. 2022;23:12928.
38. Donahue EK, Murdos A, Jakowec MW, et al. Global and regional changes in perivascular space in idiopathic and familial Parkinson's disease. *Mov Disord*. 2021;36:1126–1136.
39. Verghese JP, Terry A, de Natale ER, et al. Research evidence of the role of the glymphatic system and its potential pharmacological modulation in neurodegenerative diseases. *J Clin Med*. 2022;11.
40. Ye D, Chen S, Liu Y, et al. Mechanically manipulating glymphatic transport by ultrasound combined with microbubbles. *Proc Natl Acad Sci U S A*. 2023; 120:e2212933120.
41. Rasmussen MK, Mestre H, Nedergaard M. The glymphatic pathway in neurological disorders. *Lancet Neurol*. 2018;17:1016–1024.
42. Qin Y, He R, Chen J, et al. Neuroimaging uncovers distinct relationships of glymphatic dysfunction and motor symptoms in Parkinson's disease. *J Neurol*. 2023;270:2649–2658.
43. Iliff JJ, Lee H, Yu M, et al. Brain-wide pathway for waste clearance captured by contrast-enhanced MRI. *J Clin Invest*. 2013;123:1299–1309.
44. Ahn JH, Cho H, Kim JH, et al. Meningeal lymphatic vessels at the skull base drain cerebrospinal fluid. *Nature*. 2019;572:62–66.
45. Ringstad G, Vatnehol SAS, Eide PK. Glymphatic MRI in idiopathic normal pressure hydrocephalus. *Brain*. 2017;140:2691–2705.
46. Schonecker S, Palleis C, Franzmeier N, et al. Symptomatology in 4-repeat tauopathies is associated with data-driven topology of [(18)F]-PI-2620 tau-PET signal. *Neuroimage Clin*. 2023;38:103402.
47. Jin J, Su D, Zhang J, et al. Tau PET imaging in progressive supranuclear palsy: a systematic review and meta-analysis. *J Neurol*. 2023;270:2451–2467.
48. Kimura Y, Endo H, Ichise M, et al. A new method to quantify tau pathologies with (11)C-PBB3 PET using reference tissue voxels extracted from brain cortical gray matter. *EJNMMI Res*. 2016;6:24.
49. Zhang H, Wang M, Lu J, et al. Parametric estimation of reference signal intensity for semi-quantification of tau deposition: a Flortaucipir and [(18)F]-APN-1607 study. *Front Neurosci*. 2021;15:598234.
50. Tagai K, Ikoma Y, Endo H, et al. An optimized reference tissue method for quantification of tau protein depositions in diverse neurodegenerative disorders by PET with (18)F-PM-PBB3 ((18)F-APN-1607). *Neuroimage*. 2022; 264:119763.
51. Lu J, Clement C, Hong J, et al. Improved interpretation of 18F-florzolotau PET in progressive supranuclear palsy using a normalization-free deep-learning classifier. *iScience*. 2023;26:107426.
52. Cho H, Choi JY, Lee HS, et al. Progressive tau accumulation in Alzheimer disease: 2-year follow-up study. *J Nucl Med*. 2019;60:1611–1621.
53. Whitwell JL, Lowe VJ, Tosakulwong N, et al. [(18) F]AV-1451 tau positron emission tomography in progressive supranuclear palsy. *Mov Disord*. 2017; 32:124–133.
54. Bohr T, Hjorth PG, Holst SC, et al. The glymphatic system: current understanding and modeling. *iScience*. 2022;25:104987.
55. Sigurdsson B, Hauglund NL, Lilius TO, et al. A SPECT-based method for dynamic imaging of the glymphatic system in rats. *J Cereb Blood Flow Metab*. 2023;43:1153-1165
56. Jiang D, Liu L, Kong Y, et al. Regional glymphatic abnormality in behavioral variant frontotemporal dementia. *Ann Neurol*. 2023;94:442–456.
57. Fiorenzato E, Weis L, Falup-Pecurariu C, et al. Montreal cognitive assessment (MoCA) and Mini-mental state examination (MMSE) performance in progressive supranuclear palsy and multiple system atrophy. *J Neural Transm (Vienna)*. 2016;123:1435–1442.

Downloaded from http://journals.lww.com/nuclearmed by BhDMf5ePHKav1zEoum1tQfN4a+kJLhEZgbsIHo4XMi0hCywCX1AWnYQp/IlQrHD3i3D0OdRyi7TvSFl4Cf3VC4/OAVpDDa8K2+Ya6H515kE= on 04/11/2024

© 2024 The Author(s). Published by Wolters Kluwer Health, Inc.